Epilepsia, **44**(5):647–658, 2003
Blackwell Publishing, Inc.

Neuronal Cell Death in a Rat Model for Mesial Temporal Lobe Epilepsy Is Induced by the Initial Status Epilepticus and Not by Later Repeated Spontaneous Seizures

*†[1]Jan A. Gorter, *[1]Pedro M. Gonçalves Pereira, *Erwin A. van Vliet, †‡Eleonora Aronica, *†Fernando H. Lopes da Silva, and *Paul J. Lucassen

**Swammerdam Institute for Life Sciences, Section Neurobiology, University of Amsterdam, Amsterdam; †Stichting Epilepsie Instellingen Nederland, Heemstede; and ‡Department of (Neuro)Pathology, Academic Medical Center, University of Amsterdam, Amsterdam, The Netherlands*

Summary: *Purpose:* To determine whether repeated seizures contribute to hippocampal sclerosis, we investigated whether cell loss in the (para) hippocampal region was related to the severity of chronic seizure activity in a rat model for temporal lobe epilepsy (TLE).

Methods: Chronic epilepsy developed after status epilepticus (SE) that was electrically induced 3–5 months before. The presence of neuronal damage was assessed by using Fluoro-Jade and dUTP nick end-labeling (TUNEL) of brain sections counterstained with Nissl.

Results: We found a negative correlation between the numbers of surviving hilar cells and the duration of the SE ($r = -0.66$; $p < 0.01$). In the chronic phase, we could discriminate between rats with occasional seizures (0.15 ± 0.05 seizures per day) without progression and rats with progressive seizure activity (8.9 ± 2.8 seizures/day). In both groups, the number of TUNEL-positive cells in parahippocampal regions was similar and higher than in controls. In the hippocampal formation, this was not significantly different from controls. Fluoro-Jade staining showed essentially the same pattern at 1 week and no positive neurons in chronic epileptic rats.

Conclusions: Cell death in this rat model is related to the initial SE rather than to the frequency of spontaneous seizures. These results emphasize that it is of crucial importance to stop the SE as soon as possible to prevent extended cell loss and further progression of the disease. They also suggest that neuroprotectants can be useful during the first week after SE, but will not be very useful in the chronic epileptic phase. **Key Words:** Necrosis—Apoptosis—Parahippocampal region—TUNEL—Fluoro-Jade—Sclerosis—Epileptogenesis—Progression.

Since the discovery that a specific neuropathologic syndrome of temporal lobe epilepsy (TLE) is associated with hippocampal mesial sclerosis, there has been a controversy whether the sclerosis is the cause or consequence of repeated complex partial seizures [reviewed in (1,2)]. Various reports on experimental TLE models, in particular the kindling model, suggest that repeated seizures cause progressive hippocampal damage (3,4). However, the kindling model is a model for repeated seizures in which seizures are triggered by electrical stimulation, whereas spontaneous seizures are rarely recorded. Moreover, kindling-induced damage is relatively mild, and the claim of cell loss due to repeated seizures is not always confirmed when cell densities are taken into account (5,6). Previous research in animal models in which chronic seizures developed after a pharmacologically or electrically induced status epilepticus (SE) have shown that extensive cell death occurs almost immediately after the SE in various brain regions (7–9). However, studies that investigated the effects of chronic seizures on cell death have relied mainly on morphologic/stereologic measurements (10,11), so that subtle seizure-induced cell loss might have remained undetected.

In this study we used the post-SE model in which an SE was induced by electrical stimulation of the angular bundle (12). By using continuous hippocampal EEG monitoring, we reported previously that the SE can produce two types of epileptic evolutions in the rats: (a) epileptic rats that display an increasing number of seizures after a latent period, called "progressive post-SE rats" (p-SE); and (b) epileptic rats that display only occasional spontaneous seizures without an increase in seizure frequency for ≥5 months after the SE, called

Accepted December 14, 2002.
Address correspondence and reprint requests to Dr. J. A. Gorter at Kruislaan 320, 1098 SM, Amsterdam, The Netherlands. E-mail: gorter@science.uva.nl
[1]Co-first authors for citation purposes.

"nonprogressive post-SE rats" (np-SE) (12). These two different groups offer the possibility to test the hypothesis that the number and frequency of spontaneous recurring seizures contribute to cell loss.

To investigate whether repeated spontaneous seizures contribute to the specific neuropathology, we used two different markers to detect neuronal loss/damage in combination with cell density counts (Nissl stain): terminal deoxynucleotidyl transferase–mediated biotinylated UTP nick end-labeling (TUNEL), which identifies apoptotic and necrotic neurons in situ, and Fluoro-Jade (FJ) staining that shows degenerating neuronal cells (13). With these methods, we determined the spatiotemporal relation between the extent of cell death during the chronic epileptic phase and the frequency of seizures on the one hand, and the duration of the initial SE, on the other.

MATERIALS AND METHODS

Experimental animals

Male Sprague–Dawley rats (Harlan CPB laboratories, The Netherlands) weighing 350–450 g were used in this study. The rats were housed in individual cages under a controlled environment (21 ± 1°C; humidity, 60%; lights on, 08.00–20.00 h). Food and water were available ad libitum. To record hippocampal EEG and to stimulate the angular bundle, a pair of insulated stainless steel electrodes was implanted under electrophysiologic control by using the following coordinates: 3.9 mm anterior–posterior (AP), −3.5 mm dorsoventral 1.7 mm mediolateral, nosebar –3.9 mm, for recording. For stimulation of the angular bundle, a pair of stainless steel electrodes was implanted (7.2 mm AP, 4.5 mm mediolateral). After the electrode implantation, the rats were individually housed for ≥2 weeks to recover from the operation. The rats were then transferred to the EEG recording cage, and a week after habituation to the new condition, the rats underwent a series of tetanic stimulations (50 Hz) of the hippocampus in the form of a succession of trains of pulses, each of 13 s. Each train had a duration of 10 s and consisted of biphasic pulses (pulse duration, 0.5 ms; maximal intensity, 500 μA), similar to the protocol of Lothman et al. (14). During the electrical stimulation, the behavior of the rat was observed, and stimulation was stopped when the rats displayed sustained forelimb clonus and strong salivation for minutes. This behavioral condition was usually reached within 1 h; if not, stimulation was continued, but it never lasted >90 min.

Differential hippocampal EEG signals were amplified (10×) via an FET transistor that connected the headset to an amplifier (50×; CyberAmp; Axon Instruments, Burlingame, CA, U.S.A.), filtered (1–60 Hz) and digitized by a Pentium computer. A seizure-detection program (Harmonie; Stellate Systems, Montreal, Quebec, Canada) sampled the incoming signal at a frequency of 200 Hz per channel, but because seizures were sometimes missed by automatic detection software, we recorded the EEG continuously. Every 24 h, recordings were interrupted briefly to transfer previous day's recordings to a central review computer. EEG recordings were reviewed afterward to quantify seizure frequency and seizure duration and stored on compact disks; this procedure was repeated daily until the rats were killed for histologic and immunocytochemical processing. The length of the electrographic seizures was measured by using the duration cursor in "Reviewer" software (Stellate Systems). Additional information concerning behavioral seizure activity was obtained by using video-monitoring. Days before killing, a video recording was made of each rat during 6 h, and the behavior during an electrographic seizure was scored according to the scale of Racine (15). Behavioral scoring also was performed when seizures were observed during the daily transfer of EEG recordings.

Usually, immediately after the termination of the stimulation, periodic epileptiform discharges (PEDs) at a frequency of 1–2 Hz were evident in the hippocampal EEG. If these rats displayed PEDs for ≥4 h without interruption after the electrical stimulation, we considered that the rats belonged to the SE group. Note that we did not include in this definition a criterion regarding the occurrence of behavioral seizures, because the latter could have a variety of forms of appearance whereas the EEG criterion was more reliable. Rats were intraperitoneally injected with pentobarbital (Nembutal; Sanofi Santé B.V, France; 60 mg/kg) 4 h after termination of the tetanic stimuli to avoid a severe and prolonged SE possibly leading to death. After recovery from the anesthesia (1–2 h), PEDs could still continue for many hours, but at this time, rats only showed several behavioral seizures. Rats in which the electrical stimulation did not induce SE were defined as belonging to the non-SE group. These rats experienced several stage IV–V seizures during stimulation but not immediately thereafter; after a latent period of about a month, a seizure is registered occasionally (12). Sham-operated electrode-implanted control rats (n = 11) were handled in the same way but not stimulated. The experimental protocols followed the European Communities Council directive 86/609/EEC and the Dutch Experiments on Animal Act (1997) and were approved by the University welfare committee.

Tissue preparation

At 4 h (n = 1 SE; 1 non-SE), 24 h (n = 6 SE; n = 4 non-SE), 48 h (n = 6 SE; n = 4 non-SE), 1 week (n = 7 SE; n = 4 non-SE), 4 weeks (n = 1 SE), 6 weeks (n = 3 SE), and 3–5 months (n = 25 SE; n = 5 non-SE) after electrical stimulation, rats were anaesthetized with pentobarbital (Nembutal, Sanofi Santé B.V., France; 60 mg/kg) and perfusion-fixed through the ascending aorta

with 0.37% Na_2S solution followed by perfusion of 4% paraformaldehyde in 0.1 *M* phosphate buffer (PB) and 0.2% glutaraldehyde (pH 7.4). After in situ postfixation overnight (at 4°C), the brains were dissected and transferred to 30% sucrose in PB. After one night at +4°C, the brains were dissected into two halves by a cut along the interhemispheric fissure and frozen at −20°C to −30°C in 2-methylbutane. Ipsilateral and contralateral midbrains were stored separately at −80°C. Age-matched sham-operated controls (n = 11) underwent the same procedures. Ipsilateral brain sections were cut on a cryostat at 20 μm and pasted directly onto glass slides (SuperFrost Plus; Menzel-Glaser, Merck, Amsterdam, Holland) and stored at −80°C until use. Contralateral sections were cut at 40 μm on a sliding microtome and stored in glycerol/DMSO at −25°C. Both sides were used for TUNEL and immunostaining. Counts at the contralateral site were corrected for section thickness by using a correction factor based on the control counts (i.e., the number of cells counted in the hilar region on Nissl stain at ipsilateral site divided by the contralateral site count).

TUNEL staining

To identify dying cells, TUNEL staining was applied on tissue sections from dorsal (−4.10 mm to −4.60 mm relative to bregma) and ventral (−6.82 mm to −7.34 mm) horizontal levels of the hippocampus, as described previously with minor modifications (16,17). Prostate sections of a castrated Wistar rat were included as positive control (18). In brief, after a short wash in 0.1 *M* PB, pH 7.4, mounted sections were placed in plastic jars, filled with 0.05 *M* citrate buffer, pH 6.0, and pretreated in a microwave oven for 5 min at 800 W, after which the jars were allowed to cool for 20 min (19). Slides were then washed twice with 0.01 *M* PB saline (PBS), pH 7.2, and preincubated in proteinase K (PK) buffer (10 m*M* Tris/HCl; 2.6 m*M* $CaCl_2$; pH 7.0), followed by 20 μg/ml PK (Sigma Aldrich, Zwijndrecht, Holland) in PK buffer for 15 min at room temperature (RT), washed and incubated with terminal deoxynucleotidyl transferase (TdT) buffer (1 *M* sodium cacodylate, 0.125 *M* Tris/HCl in 1.25 mg/ml bovine serum albumin (BSA); pH 6.6) for 15 min at RT before incubation for 60 min at 37°C in TdT buffer, containing per 100 μl, 0.2 μl TdT (Boehringer Mannheim, Germany), 0.5 μl biotin-16-dUTP (Boehringer Mannheim, Germany), and cobalt chloride (25 mmol; 5% of the final volume). After rinsing in PBS (pH 7.4), endogenous peroxidase was blocked with 3% hydrogen peroxide (H_2O_2) in PBS, and sections were preincubated with PBS/1% BSA before peroxidase-conjugated avidin (ABC-Elite kit; Vector Laboratories, Inc., Burlingame, CA, U.S.A.) 1:1,000 in PBS/1% BSA for 1.5 h at RT. Labeled DNA was visualized with 10 mg/ml diaminobenzidine (DAB; Sigma Aldrich, Zwijndrecht, Holland) in 0.05 *M* Tris/HCl (pH 7.5) with 0.02% H_2O_2, during which DAB development was monitored continuously. Sections were then washed and counterstained with cresyl violet.

Fluoro-Jade staining

Horizontal sections of control (n = 4), 1 week (n = 5), 6 weeks (n = 3), and 3–5 months post-SE rats (n = 8) and non-SE rats (n = 4) were stained with FJ by using the method described by Schmued et al. (13). Sections were mounted onto Superfrost Plus slides and dried overnight (37°C). They were immersed in absolute alcohol for 3 min followed by 70% ethanol for 1 min and distilled water for 1 min. The slides were transferred to 0.06% potassium permanganate for 15 min. After rinsing with distilled water (1 min), the slides were transferred to a 0.001% FJ solution (Histo-Chem, Inc., Jefferson, AR, U.S.A.) made in 0.1% acetic acid. Slides were rinsed in water, dried at 37°C, immersed in xylene, and coverslipped with entallan. Sections were analyzed with a laser scanning confocal microscope (Bio-Rad, MRC1024, Hercules, CA, U.S.A.).

Double immunofluorescence

To reveal the cellular identity, a subset of free-floating sections was double labeled by using fluorescent TUNEL that followed incubation with primary antibodies (Abs) against glial fibrillary acidic protein (GFAP; monoclonal mouse, Boehringer Mannheim, Germany; 1:500) as astrocyte marker, anti-rat CD11b/c (monoclonal mouse, OX42; Pharmingen, CA, U.S.A.; 1:100) as microglia marker, and NeuN (Mouse clone MAB377; Chemicon, Temecula, CA, U.S.A.; 1:1,000 all in PBS-BSA + 0.1% Triton) as neuronal marker.

Fluorescent TUNEL was identical as described earlier, except for the biotin-16-dUTP that was replaced with fluorescein-12-deoxy-UTP (Boehringer) and the TdT and PK concentrations were reduced to 50%. Primary antibodies were incubated overnight, and after washing, sections were incubated with CY3 goat anti-mouse immunoglobulin G (IgG) antisera (Zymed, San Francisco, CA, U.S.A.; 1:200), washed and mounted on Superfrost Plus slides for subsequent TUNEL staining. Sections were embedded in Vectashield and analyzed with a laser scanning confocal microscope (Bio-Rad, MRC1024, Hercules, CA, U.S.A.) equipped with argon-ion laser. In a subset of sections, we used NeuN (as neuronal marker) or OX42 (as microglial marker) immunostaining (with CY3 goat anti-mouse IgG antisera (Zymed, San Francisco, CA, U.S.A.; 1:200) followed by incubation with FJ.

Quantification of neuronal loss (Nissl stain)

The extent of structural cell loss in Nissl-stained sections in various brain regions of the ipsilateral and contralateral hemispheres was assessed at ×400 magnification by using grid morphometric techniques. Two sections per rat and per level (dorsal, ventral) were quantified. To avoid confusion with glial cells, neurons were

defined as profiles >10 μm (hilus) or 7 μm (cortex) having an identifiable nucleolus. An ocular grid consisting of 5 × 5 box segments (240 × 240 μm), was placed over the region of interest. For the entorhinal cortex (EC) layer, the medial part was analysed (mEC). Boundaries of each region were taken from the recent description of the hippocampal formation (20). The anterior piriform cortex was evaluated at the ventral level (–7.1 mm to –7.4 mm relative to bregma; see also diagram in Fig. 3E). Layer II, III, dorsal endopiriform nucleus, and claustrum were separately analyzed. For the different cortical layers, a linear 1 × 5 box was used. Typically nearly all of any specific layer would be included in the field. For hilar cell counts, a slightly different technique was used. To express the results as cell densities, we measured the hilar area by using Scion Image software (Scion Corporation, Maryland, U.S.A.) over digital images (camera HCS MXR Vision Technology, The Netherlands). The hilus was defined as the inner border of the granule cell layer (GCL) together with the area formed by two imaginary straight lines connecting the two tips of the GCL with the proximal end of the CA3c area. The number of hilar neurons was counted at ×200 magnification. Final neuron counts were calculated as the number of neurons per square millimeter. It should be emphasized that our neuron-counting methods are relative estimates and not absolute calculations of the number of hippocampal (parahippocampal, etc.) neurons. The neuron counts as used in this study can be considered reliable relative estimates at the specific dorsal and ventral level. Statistical differences in neuron counts between groups of animals can be accurately determined.

Quantification of TUNEL-positive cells

TUNEL-positive cells were quantified in the different hippocampal subfields as well as in the parahippocampal region and anterior piriform cortex (layer II, layer III, and dorsal endopiriform nucleus) of both hemispheres. Quantification was performed at ×400 magnification with a microscope rectangular grid. Two sections per level and per rat were analyzed. To account for tissue changes (swelling and/or shrinking), we measured the areas of the different regions (hippocampus, hilus, and the parahippocampal region) by using Scion Image software. TUNEL-positive cell numbers were then expressed as densities per region. Because the number of TUNEL-positive cells was very low in control and chronic epileptic rats, the number of cells also was expressed per region in a dorsal/ventral section. The parahippocampal area included the presubiculum, parasubiculum, the six-layered medial and lateral entorhinal cortex (mEC and lEC). Within the hippocampus, TUNEL cell counts were performed in the DG, CA1-3, and subiculum. To obtain the local distribution of TUNEL-positive cells in hippocampal and parahippocampal region and anterior piriform cortex, the labeled cells were plotted from sections with the aid of camera lucida and drawn in diagrams obtained from *The Rat Brain* atlas (21). In several rats, TUNEL distributions were compared with a FJ stain distribution in a consecutive brain section.

Statistics

Mean values and SEMs were calculated. Differences in mean values were determined by use of one-way analysis of variance (ANOVA) followed by a post hoc test (Bonferroni, $p < 0.05$) or Kruskal–Wallis test followed by a Mann–Whitney test ($p < 0.05$). Statistics were determined from the raw data. Data on cell densities were normalized to the control densities (100%); a correlation between two ordinal variables was calculated by using a Spearman rank correlation test ($p < 0.01$) with statistics software (SPSS, Inc., for Windows, release 10).

RESULTS

Relation between duration of the SE and neurons in the hilar region

The SE was stopped after 4 h, but PEDs reappeared again after some time and could continue for several hours afterward. SE duration was quantified based on the duration of the period during which PEDs occurred in 17 rats that had developed a progressive form of epilepsy (p-SE rats; six of which were submitted to TUNEL evaluation) and in nine rats that had developed a non-progressive form of epilepsy (np-SE rats; seven of which were evaluated with TUNEL) starting after the stimulation was stopped. The SE duration and number of daily seizures (during the last 2 weeks of EEG recording before killing) for individual p-SE and np-SE rats are indicated in Fig. 1A; the corresponding mean SE duration for each group is indicated in the inset. The average SE duration appeared to last 1.7 times longer in p-SE rats (7.0 ± 1.1 hs in np-SE and 11.8 ± 0.9 h in p-SE rats; Student's t, $p < 0.001$). The average duration of an individual seizure also was measured. During the last 2 weeks before killing, seizures lasted at average ~1 min, (72 ± 4 in np-SE rats and 58 ± 5 s in p-SE rats; $p < 0.01$). In chronic epileptic rats, at 3–5 months after SE, Nissl cell counts indicated that there was a significant negative correlation between the number of hilar cells and the duration of the SE (Fig. 1B; Spearman rank correlation, $r = -0.66$; $p < 0.01$).

Nissl densities in hippocampal and extrahippocampal regions

First we evaluated cell loss quantitatively by analyzing Nissl cell densities in selective hippocampal and extrahippocampal regions at different times after the SE. More specifically, we analyzed the hilus at dorsal and ventral levels, mEC layers II, III, and V/VI at the ventral level, and anterior piriform cortex including dorsal endopiriform nucleus and claustrum at the ventral level.

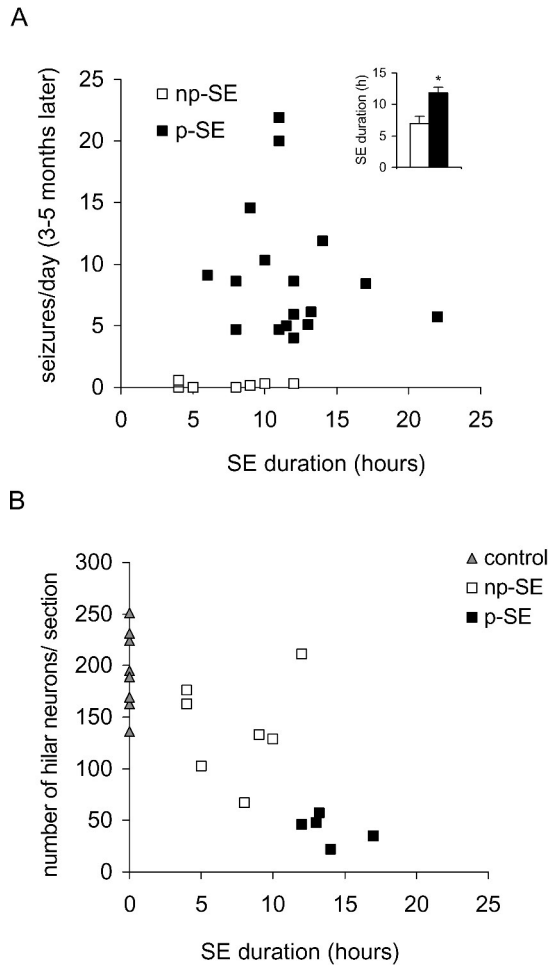

FIG. 1. **A:** Relation between the duration of the status epilepticus (SE) and the later individual seizure activity in progressive epileptic rats (solid squares) and nonprogressive epileptic rats (open squares) during the last 2 weeks before perfusion. The average group data (inset 1A) indicate that rats with a progressive form of epilepsy had a significant longer SE than did rats with a nonprogressive form of epilepsy. **B:** Relation between the duration of the SE and the number of hilar Nissl cells at dorsal hippocampus after SE. There is a significant negative correlation ($r = -0.66$; $p < 0.01$) between the duration of the SE and the hilar cell number of the three groups.

Figure 2 shows changes in Nissl cell counts after SE on the ipsilateral site. There was a dramatic reduction in Nissl cell density within 1–2 days after SE at the ipsilateral hilus (A), mEC layer II/III (C), and layer II of the piriform cortex including the dorsal endopiriform nucleus/claustrum (E). Layers V/VI of the mEC and the deep layer of the piriform cortex were not significantly affected at this ventral level (7.1–7.4 mm below bregma). At more ventral levels, all piriform cortical layers (anterior and posterior) were very severely affected and almost completely filled with vimentin-positive astrocytes (not shown). These Nissl density measurements suggested that cell loss did not increase further beyond 1 week after SE. In other areas including the midline thalamic nuclei, perirhinal cortex, septal areas, and amygdaloid nuclei, cell loss was also observed during the earlier time points, but these areas were not further analyzed in detail. On the contralateral side, cell-density changes were essentially the same or slightly less than observed ipsilaterally, except in the hilus and piriform cortex, in which the reduction of cell density was far less dramatic in rats that had developed a nonprogressive form of epilepsy versus rats with a progressive form of epilepsy [see also (12)]. In sections of non-SE rats, no significant change in cell density was observed in the entorhinal cortex (not shown) and piriform cortex (Fig. 2F).

Evolution of TUNEL/Fluoro-Jade staining in hippocampal and extrahippocampal regions after SE

TUNEL analysis in hippocampal and parahippocampal regions of controls revealed only a few positive cells. In stimulated rats, TUNEL cell numbers varied considerably over time, as did their morphology. During the first week, cells that were TUNEL positive showed mainly a shrunken morphology, whereas at later times (>3 months), the few cells that were TUNEL positive revealed sometimes apoptotic bodies. All TUNEL cells were quantified irrespective of their morphologic appearance. As indicated in Fig. 3A and B, TUNEL cell numbers were already robustly increased at 1 day after stimulation. The numbers reached a peak within 1 week after SE in all subregions of the hippocampus. After that, TUNEL cell numbers dramatically decreased. No significant difference was seen between the amount of stained cells at the dorsal and the ventral levels of the hippocampus or between ipsi- and contralateral sides (data not shown). Examples of the TUNEL labeling are shown in Fig. 4A (gcl, control) and 4B and C (CA3, CA1, 1 week after SE). In chronic epileptic rats (3–5 months after SE), the number of TUNEL cells in the hippocampus was low and not statistically different from that in control rats. In rats that had not experienced SE (non-SE rats), there was a small but nonsignificant increase of TUNEL cells during the first week after SE (Fig. 3C).

TUNEL positivity in the parahippocampal region also showed a large increase during the first week after SE (Fig. 3B), but the evolution was somewhat different compared with hippocampus. Most TUNEL positivity appeared during the first days after SE. Extensive TUNEL labeling in entorhinal cortex 1 week after SE was found mainly in layer III and parasubiculum where cell loss is prominent. In the anterior piriform cortex, cell death also was extensive during the first week and more extensive in layer II than in layer III (Fig. 3E; 6B and C). In the dorsal endopiriform nucleus, TUNEL labeling was extensive during the first week (Fig. 3E).

In epileptic non-SE rats that had not experienced SE after electrical stimulation, an increase of TUNEL cells was observed in the ventral parahippocampal region dur-

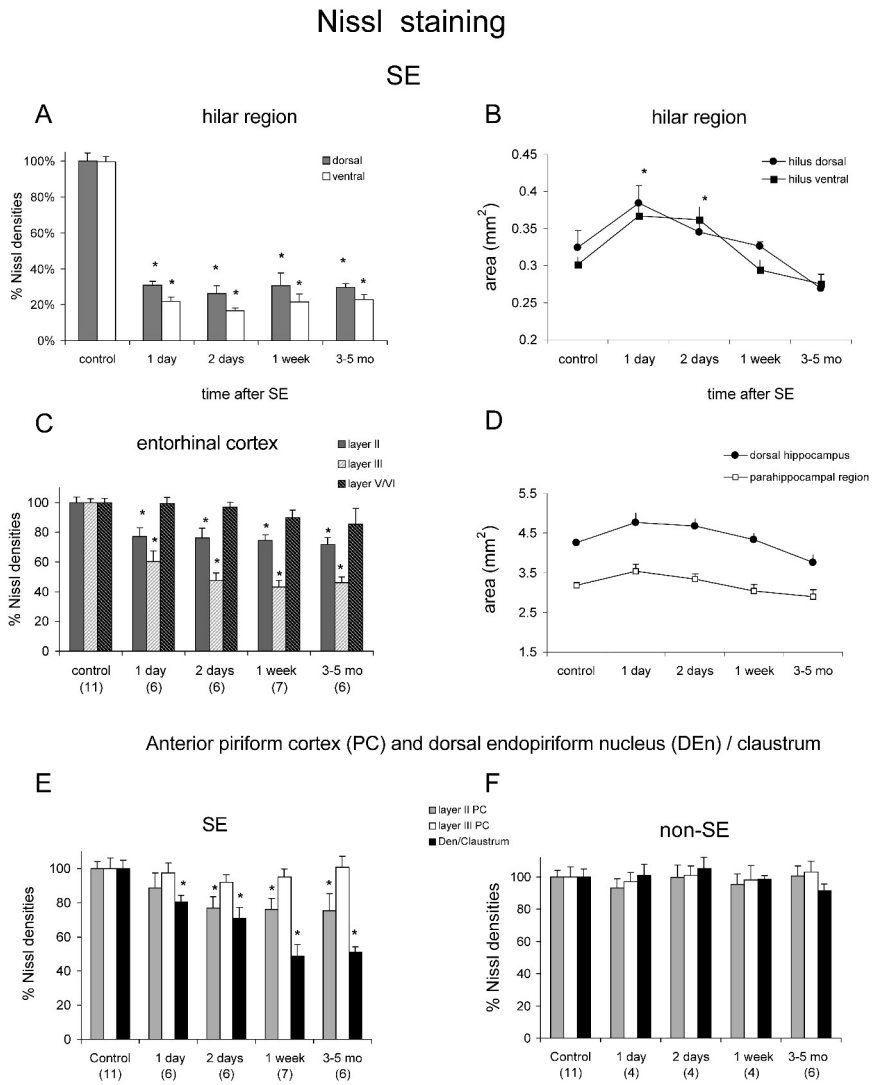

FIG. 2. Evolution of Nissl cell densities after status epilepticus (SE). **A:** Ipsilateral hilar cell densities in dorsal and ventral hippocampus. **B:** Changes in dorsal and ventral hilar surface areas after SE. **C:** Evolution of Nissl cell densities in each layer of the medial entorhinal cortex. **D:** Changes of total surface area of the hippocampus and parahippocampal region after SE. **E, F:** Changes of Nissl cell densities in layers of the anterior piriform cortex and dorsal endopiriform nucleus and claustrum in post-SE **(E)** and non-SE rats. Control densities are normalized to 100%. *Significantly different from control value; Bonferroni $p < 0.05$).

ing the first week after SE, which was significant at 1 week after stimulation (Fig. 3D). Non-SE rats did not show increased numbers of TUNEL cells at later times (3–5 months).

The fact that a large number of TUNEL cells was present during the first week after SE led us to investigate whether these cells were astrocytes or microglial cells, because particularly these cell types proliferate extensively during the first week after SE (22,23). After double immunolabeling of TUNEL with NeuN, GFAP, and OX42 (identifying neurons, astrocytes, and microglia, respectively), no double labeling could be detected for any of these markers. Reactive microglia enwrapping TUNEL-labeled cells was frequently observed (Fig. 4C).

FJ staining of brain sections of post-SE rats showed essentially the same pattern as observed with the TUNEL labeling (Compare Fig. 4B–E and 4C–F). The advantage of the FJ stain lies in the fact that the neuronal morphology still can be visualized, including dendritic processes (see, for instance, Fig. 4F and H). Despite the clear neuronal morphology, double labeling of post-SE sections with NeuN showed that FJ-positive cells were not still recognized by the antibody (e.g., Fig. 4 H and I). In the same sections, the granule neurons were NeuN positive.

Chronic seizure activity and cell death

SE can lead to distinct evolution of spontaneous seizure activity with either a progressive increase of seizure activity in 67% or a nonprogressive form in 33% of the rats (12). We investigated tissue of p-SE rats ($n = 6$) and np-SE rats ($n = 7$) and compared this with tissue of non-SE rats ($n = 2$; these also experience a nonprogressive form of epilepsy after a longer latent period) and control tissue ($n = 11$, age matched). Figure 5 shows the relation between individual seizure activity, expressed as the number of daily seizures during the last 2 weeks before perfusion, and the number of TUNEL cells encountered in hippocampal (A) and parahippocampal sec-

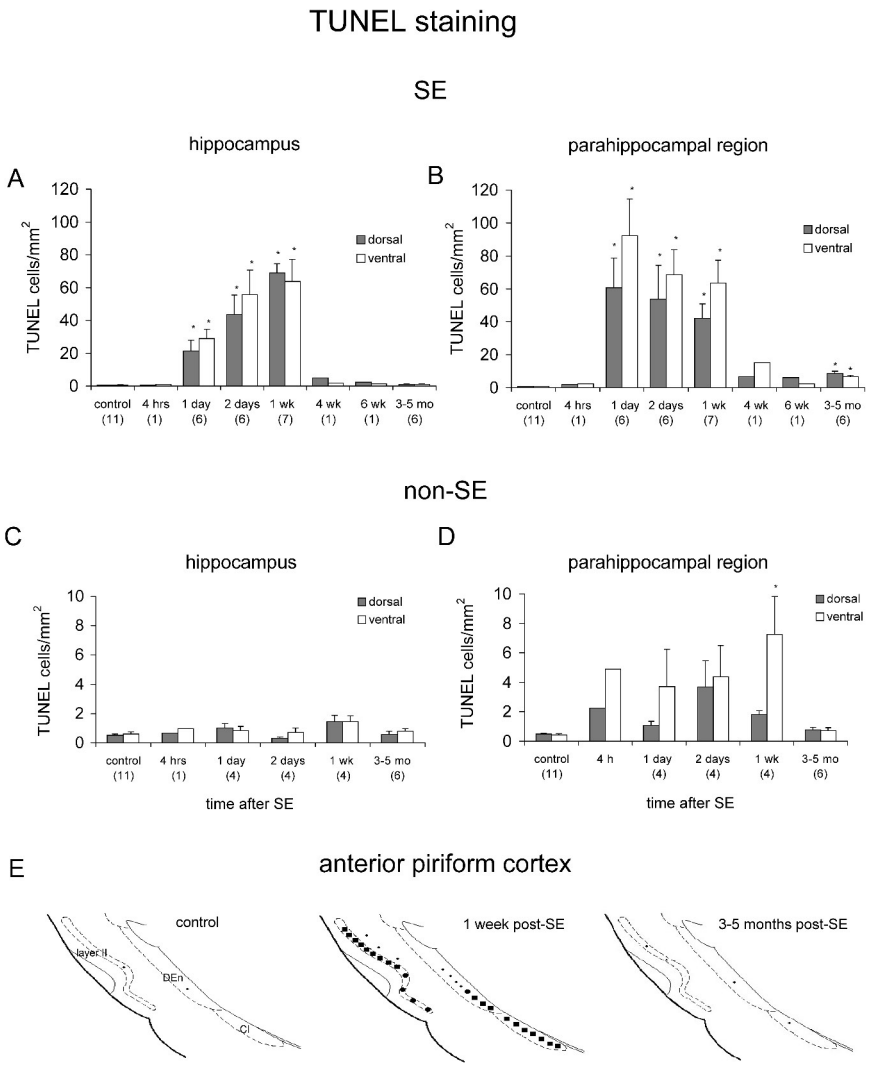

FIG. 3. Quantification of TUNEL-positive cells (TUNEL cells) in the hippocampal and parahippocampal region. **A:** Development of the pattern of TUNEL cells (expressed as density: number per mm^2) in the dorsal and ventral hippocampus (ipsilateral) at different times after status epilepticus (SE). **B:** Cell loss in the parahippocampal region occurs also during the first week but with a somewhat different pattern from that in the hippocampus. **C:** Evolution of TUNEL positivity in the hippocampal region of non-SE rats. **D:** Evolution of TUNEL positivity in the parahippocampal region of non-SE rats. During the first week after stimulation, no change is seen in the hippocampus, but an increase in TUNEL cells occurs in the parahippocampal region (note different scale compared with A, B). **E:** Schematic diagrams showing an overview of the distribution of TUNEL-positive cells in the different layers of the anterior piriform cortex and the dorsal endopiriform nucleus (Den)/claustrum (Cl). *Significantly different from control; Bonferroni $p < 0.05$).

tions (B) of the three groups (indicated with different symbols), including the control group. In the chronic phase, TUNEL cell numbers were very low, but they could be encountered in all regions including the relatively seizure-resistant GCL and presubiculum. The averages of the hippocampal and parahippocampal TUNEL-positive cell counts (here expressed as TUNEL cells per region) and several seizure-activity parameters of each group are shown in Table 1. TUNEL cells were not increased in p-SE rats with more frequent and more recent seizures compared with rats of the np-SE group. In the hippocampus, the number of TUNEL cells was quite comparable between the two epileptic post-SE groups and tended to be slightly (not significantly) higher than that in controls. In the parahippocampal region, the number of TUNEL cells was comparable for both post-SE groups but considerably higher than in controls ($p < 0.05$; Table 1). In non-SE rats that also experienced chronic seizures without progression, TUNEL cell numbers were comparable to those of controls.

FJ stain corresponded largely to the TUNEL stain, as shown by others (24,25), especially during the first weeks after SE (compare Fig. 4B and 4E). FJ stain in 6-week post-SE rats still revealed some positive cells in the CA1-3 region (Fig. 4J) and the piriform cortex (Fig. 6D). They were positioned in the pyramidal cell layer and did not colocalize with microglia (Fig. 4J). In sections of rats of >3 months, no individual neurons were labeled anywhere in the hippocampus (Fig. 4L) and parahippocampal region in dorsal and ventral brain sections. In some ventral sections, there was still increased fluorescence in piriform cortex, but individual cells with neuronal morphology were not observed. In several regions (hilus, parasubiculum), though, FJ-positive cells with astrocyte-like morphology were observed (Fig. 4K).

DISCUSSION

The new and most important finding of this study is that (para)-hippocampal cell loss is related not to the

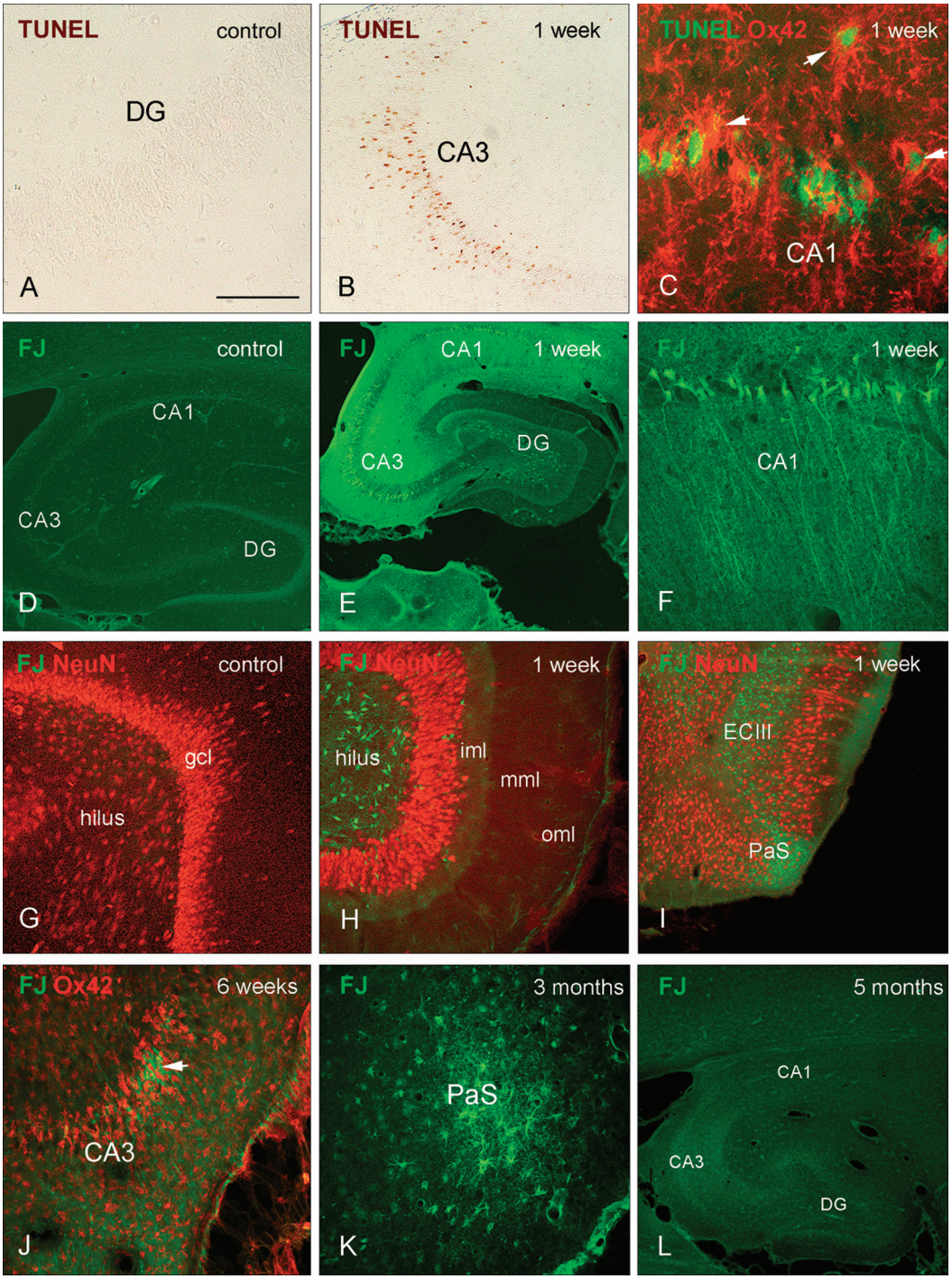

FIG. 4. Examples of TUNEL and of Fluoro-Jade (FJ) staining in (para)hippocampal sections of control rat **(A, D, G)** and rats at different times after status epilepticus (SE). **A–C:** TUNEL staining: **(A)** no labeling in control DG; **(B)** a large number of CA3 neurons are also TUNEL positive, corresponding to the FJ stain of the same 1-week post-SE rat, as shown in E. **C:** TUNEL staining in CA1 at 1 week after SE shows a fluorescent stain of OX42 (marker for microglia, in red) and TUNEL (green); white arrows indicate reactive microglia enwrapping TUNEL-labeled cells. **D–F:** Examples of an FJ stain; in a control rat **(D),** there is only a background stain. **E:** FJ stain of a hippocampal area at 1 week after SE with increased fluorescence in CA1–CA3 and hilar neurons. **F:** CA1 neurons show somatic and dendritic staining with Fluoro-Jade. **G–I:** Double labeling of FJ (green) and NeuN (red). **G:** Detail of dentate gyrus (DG) with hilar cells and granule cell layer (gcl). **H:** Details of the DG including the GCL of a 1-week post-SE rat. Note that most hilar neurons are FJ positive but do not stain for NeuN. **I:** Detail of parahippocampal region of the same 1-week post-SE rat, showing multiple FJ-positive cells in layer III of the entorhinal cortex and parasubiculum but no double labeling with NeuN. **J:** FJ-positive CA3 neurons surrounded by activated microglia at 6 weeks after SE. **K:** FJ staining in parasubiculum at 3 months post-SE with FJ-positive staining of astrocytes. **L:** FJ stain in hippocampal section of rat that displayed 12 seizures per day shows no neuronal labeling anywhere in the hippocampus. Bar in **A**, 100 μm for **A** and **K**; 200 μm for **B, F, G**, and **H, J**; 75 μm for **C**; 400 μm for **D-E, I** and **L**.

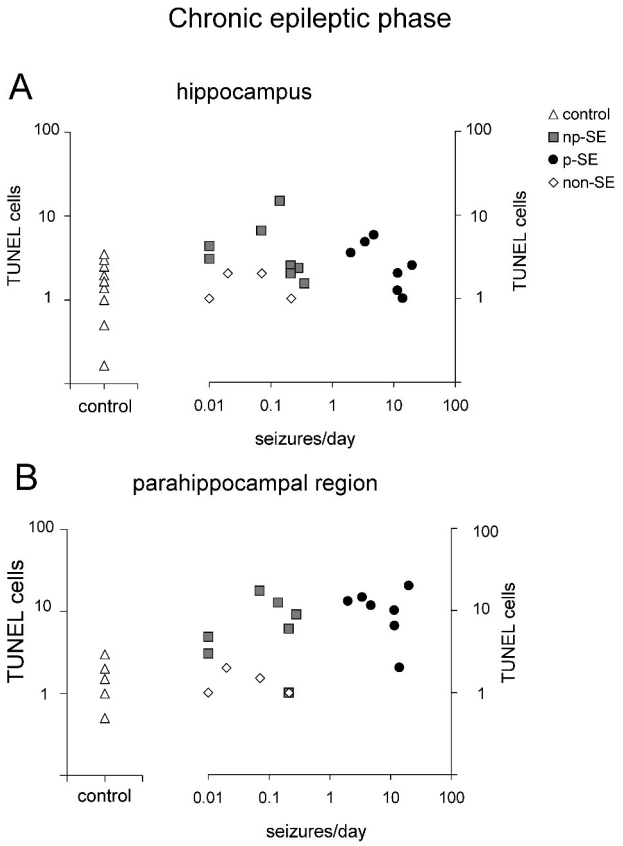

FIG. 5. Relation between individual seizure activity (expressed as seizures per day during the last 2 weeks of EEG recording) and the individual number of TUNEL cells in the dorsal hippocampus **(A)** and parahippocampal region **(B),** respectively (expressed as TUNEL cells per section). Numbers of hippocampal TUNEL cells in np-SE, p-SE, and non-SE rats overlap with controls and are not significantly different from each other. In the parahippocampal region, significantly more TUNEL cells are encountered in the np-SE and p-SE rats than in control rats (Mann–Whitney, $p < 0.05$). The two non-SE rats are in the range of controls.

frequency of spontaneously occurring seizures, but rather to the duration of the initial SE. Furthermore, we show that the majority of cells that die as a consequence of the initial SE, degenerate in the course of the first week after SE, which is in agreement with previous reports (9,26–29). Finally, the extent of hilar cell death is related to SE duration and to the later progression of the disease. These findings extend previous reports because we investigated a longer time period, including both the latent period (first week after SE) and the chronic epileptic phase (3–5 months after SE). These findings can have important implications for the management of TLE, in particular, with respect to the timing of the treatment with neuroprotectants.

Duration of status epilepticus and cell death

In our model, most TUNEL- and FJ-positive cells were encountered during the first week after SE. Cell death was more obvious in specific regions (hilus, EC layer III) but occurred in all regions investigated. A significant negative correlation was seen between the number of surviving hilar neurons and SE duration. Interestingly, rats that experienced a shorter SE appeared to have a better prognosis to develop a nonprogressive form of epilepsy (Fig. 1A). Although the exact pathway remains controversial, both apoptotic and necrotic cell death occur after SE (29–32), and cells with both apoptotic and necrotic morphology were found in our current model as well. This issue might be relevant for therapeutic intervention because neuronal degeneration could be attenuated by inhibition of caspase-3–like enzyme activity (33). The Nissl density counts indicated that the decrease in density was obtained within the first day after SE with no significant change thereafter, suggesting that cell loss beyond 1–2 days after SE is minimal. However, because the hilar area is larger at these times, indicating swelling of tissue, a considerable additional number of cells die during the first week. Even at 6 weeks after SE, a significant number of TUNEL/FJ-positive neurons were still observed. This illustrates that stereologic measurements alone are not sufficient to assess whether cell loss occurs. Our finding that the majority of degenerating cells die during the first week suggests that the time window for a possible intervention to influence the epileptogenic process could last for at least several days in this rat model.

The fact that the pattern of TUNEL-labeled cells largely corresponded with the pattern of FJ-stained cells with clear neuronal morphology emphasizes that it is likely that the majority of TUNEL-labeled cells also were neurons. We were not able to double-label these cells with glia markers in similar tissue. However, in our hands, double labeling of FJ-positive cells with NeuN also was not possible, although the cells had a clear neuronal morphology including dendritic processes (13). This may relate to the fact that TUNEL- or FJ-positive cells in this stage of their death have lost their protein markers and therefore cannot be identified by double-label immunocytochemistry. Apparently during the first week after SE, increasing and additional numbers of neurons show DNA fragmentation and are not removed immediately. In view of the high number of TUNEL-positive cells during the first week after SE, it is at least likely that these labeled cells have a more extended expression than generally thought.

Brief spontaneous seizures do not cause cell death

At first glance, the increased number of TUNEL cells encountered in p-SE rats might suggest that the occurrence of seizures indeed contributes to progression of cell death. However, this is not the case, taking into consideration the following findings: (a) rats with frequent progressive seizure activity (more than eight seizures per day) had their last seizure within several hours

TABLE 1. *Overview of important EEG parameters and the number of TUNEL-positive cells in the dorsal and ventral hippocampal and parahippocampal region sections*

	n	Days after SE	Lifetime seizures	Seizures/day last 2 wk	Time since last seizure (d)	TUNEL cells dorsal hippocampal section	TUNEL cells ventral hippocampal section	TUNEL cells dorsal parahippocampal section	TUNEL cells ventral parahippocampal section
Control	8	—	0	0	—	1.9 (0.5–3.5)	1.2 (0–2)	1.4 (0.5–3)	0.9 (0–1.5)
Non-SE	2	157.5 ± 7.5	16.0 ± 2.0	0.14 ± 0.07	6.32 ± 3.21	1.5 (1–2)	2.25 (2–2.5)	1.25 (1–1.5)	1.75 (1–2.5)
np-SE	7	111.4 ± 9.7	22.1 ± 6.7	0.15 ± 0.05	20.4 ± 15.8	5.0 (2.5–15)	3.3 (0.5–6)	8.8 (3–17.5)[b]	5.7 (3–10)[b]
p-SE	6	104.7 ± 7.8	557 ± 178[a]	8.9 ± 2.8[a]	0.14 ± 0.07[a]	3.3 (1.5–6)	4.1 (1.5–12)	11.1 (6.5–20)[b]	10.2 (4.5–16)[b]

Ipsi- and contralateral site are pooled and expressed as cells per region. Ranges of cell counts are indicated between brackets. Statistical comparisons of seizure parameters are made between np-SE and p-SE groups (Student's t, [a]$p < 0.01$). Statistical comparisons of TUNEL data are made between np-SE or p-SE group and the control group (Mann–Whitney, [b]$p < 0.05$).

before perfusion. Nevertheless they did not have more TUNEL-positive cells in the hippocampal or parahippocampal region than did rats that had their last seizure several days before perfusion (Table 1), with on average only one to two seizures per week; (b) rats that had not had SE (non-SE) showed significantly fewer TUNEL cells in these areas than did either of the post-SE groups, although they had had a comparable number of seizures during their lifetime to those of the np-SE rats; (c) with FJ, we did not observe any positively labeled neurons in rats at >3 months, suggesting that the TUNEL-positive cell counts may include some nonneuronal elements as well. These data indicate that the increased TUNEL labeling is a consequence of the aftermath of the SE and not of the individual seizure activity. The FJ staining strengthens this conclusion even more, because no individually damaged neurons were found in 3–5 months post-SE rats. Because the window for which the cells would be TUNEL/FJ-positive may be only a few hours, one could argue that we have missed ongoing cell death because of the limited sampling of TUNEL- and/or FJ-positive neurons in the chronic epileptic phase. However, the fact that rats with progressive seizure activity had an average 8.9 seizures per day (Table 1) means that the mean interval between seizures was 2.7 h. Nevertheless, the rats did not show increased positivity in comparison

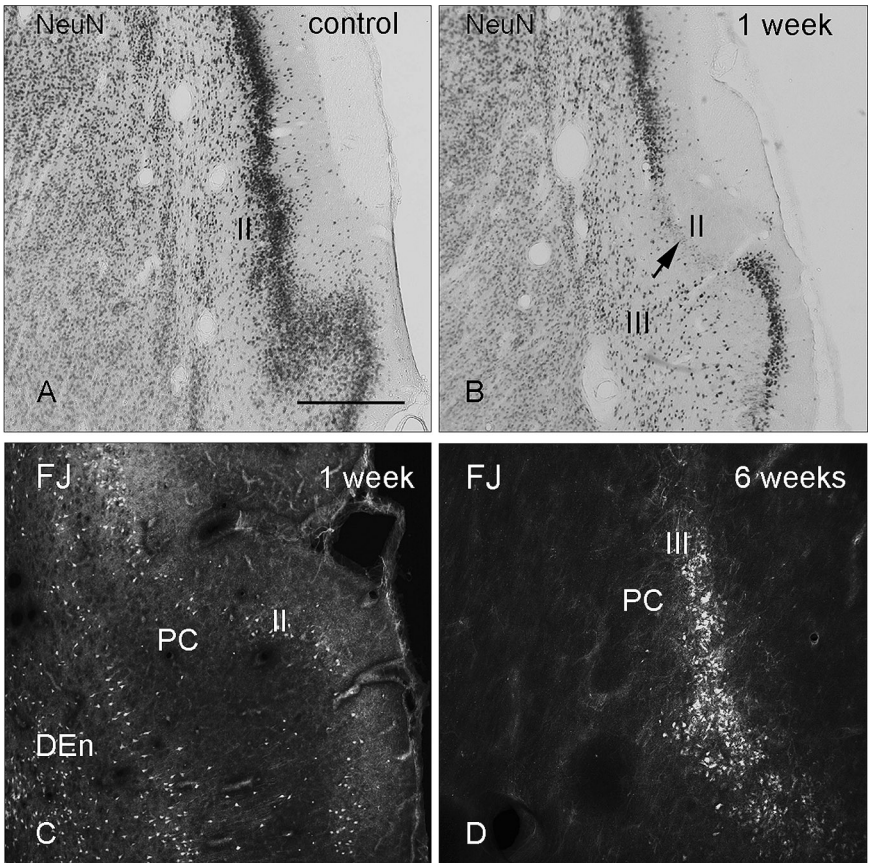

FIG. 6. Immunostaining for neuronal marker NeuN in anterior piriform cortex in control **(A)** and 1-week post-status epilepticus (SE) rat **(B).** Arrow, extensive cell loss. **C:** Fluoro-Jade (FJ) staining of anterior piriform cortex showing labeling of layer II and dorsal endopiriform nucleus at 1 week after SE. **D:** FJ labeling of layer II/III of the piriform cortex 6 weeks after SE. Calibration bar in **A:** 500 μm in **A, B**, and 100 μm in **C** and **D**.

to rats that had their last seizure several days before death ("nonprogressive"). Therefore we think that it is not very likely that TUNEL/FJ positivity could have been missed because of a too-long time interval after the last seizure. Moreover, the fact that we did not find a further decrease in neuronal densities argues also against this point. Our data contrast to what has been reported in pilocarpine-treated rats, in which rats with multiple seizures had more damaged neurons than did animals with single seizures (34). This discrepancy might be related to the different staining technique or to other factors (shorter time window after the initial SE used in the latter study). However, our findings are in agreement with a recent study that appeared during revision of our article, in which similar staining techniques were used in tissue of chronic epileptic rats (35). Cell damage 2 months after kainate-induced SE also was observed in CA1, thalamus, and piriform cortex, using the FJ B staining method (36). At this time, we still found increased fluorescence in piriform cortex, but individual cells with neuronal morphology could not be discriminated. Astrocytes in severely affected regions such as hilus and parasubiculum also showed increased fluorescence. This might reflect astrocytic activation (36).

Our findings show that the extent of cell death in the chronic epileptic phase in our rat model is not related to the frequency of spontaneous seizures. Previous studies had indicated that electrically evoked seizures actually cause progressive cell loss, suggesting that hippocampal sclerosis in human epilepsy may be acquired as a consequence of repeated seizures (2,3,37,38). Apparently neurons are more sensitive to seizures evoked by electrical stimulation than to spontaneously occurring seizures. However, the previously published kindling studies associated neuronal loss with stage 5 or greater seizures. These are very robust significant seizures with secondary generalization and perhaps secondary hypoxic ischemia during the events. In humans, an association with hippocampal neuronal loss and the presence of secondarily generalized seizures was found (39). In all rats that we included in this study, we observed generalized tonic–clonic seizures [stage 4–5 on the scale of (15)] during the chronic epileptic phase, although partial seizures also were observed. Therefore, we cannot exclude that the difference between these studies may relate to the severity of the evoked or spontaneous seizure. Our present findings indicate that seizures do not lead to cell death when they occur spontaneously and are generalized with restricted duration (on average, 1–2 min). This suggests that the sclerosis is likely related to events other than the frequency of spontaneous seizures. Accordingly, it is possible that in human patients, hippocampal sclerosis is induced by a previous brain insult or by some kind of predisposition. This latter possibility is supported by the observation of a preexisting hippocampal lesion, as encountered by using magnetic resonance imaging (MRI) studies in humans (40,41).

Notwithstanding these observations, several longitudinal MRI studies suggested that a progressive decrease of hippocampal volume may result from the cumulative effect of brief recurrent seizures in humans (42–45) and in pilocarpine-treated rats (46). Nevertheless, a decrease in hippocampal volume was found in only four of 33 epilepsy patients in a 3.5-year follow-up study (47). Moreover, it must be realized that a reduction in volume does not necessarily indicate neuronal loss. Shrinkage of neurons and surrounding cells could also contribute to the observed volume reductions. In addition, it is not clear from patient studies whether the TLE syndrome is the only underlying etiology and/or whether medication can have an effect on hippocampal volumes. We should note that the duration of the epilepsy in the rat model is quite different from that in the human. Although the time scales are very different, we may assume that a 3- to 5-month post-SE rat is comparable with a patient that has TLE for a couple of years.

CONCLUSIONS

In conclusion, our data indicate that cell death is not related to seizure frequency when seizures occur spontaneously and are of restricted duration. Therefore it is unlikely that drugs that interfere with cell-death pathways or reorganization will be of any use at the chronic epileptic phase, if seizures are relatively short (<2 min). These data emphasize the importance of an early intervention directed to minimize the effects of SE to prevent progression of epilepsy.

Acknowledgment: We thank S. Maslam for histologic assistance. Grant sponsors: Nationaal Epilepsie Fonds "Power of the Small"; grant 20-03 and 03-03 (J.A.G. and E.A.V.) and Fundação para a Ciência e a Tecnologia BD 18498/98 of Portugal (P.M.G.P.), Dutch Organization for Scientific Research (NWO) (P.J.L.).

REFERENCES

1. Mathern GW, Babb TL, Leite JP, et al. The pathogenic and progressive features of chronic human hippocampal epilepsy. *Epilepsy Res* 1996;26:151–61.
2. Sutula TP, Pitkanen A. More evidence for seizure-induced neuron loss: is hippocampal sclerosis both cause and effect of epilepsy? *Neurology* 2001;57:169–70.
3. Bengzon J, Kokaia Z, Elmer E, et al. Apoptosis and proliferation of dentate gyrus neurons after single and intermittent limbic seizures. *Proc Natl Acad Sci U S A* 1997;94:10432–7.
4. Cavazos JE, Das I, Sutula TP. Neuronal loss induced in limbic pathways by kindling: evidence for induction of hippocampal sclerosis by repeated brief seizures. *J Neurosci* 1994;14:3106–21.
5. Bertram EH, Lothman EW. Morphometric effects of intermittent kindled seizures and limbic status epilepticus in the dentate gyrus of the rat. *Brain Res* 1993;603:25–31.
6. Adams B, Sazgar M, Osehobo P, et al. Nerve growth factor accelerates seizure development, enhances mossy fiber sprouting, and

attenuates seizure-induced decreases in neuronal density in the kindling model of epilepsy. *J Neurosci* 1997;17:5288–96.
7. Schwob JE, Fuller T, Price JL, et al. Widespread patterns of neuronal damage following systemic or intracerebral injections of kainic acid: a histological study. *Neuroscience* 1980;5:991–1014.
8. Nevander G, Ingvar M, Auer R, et al. Status epilepticus in well-oxygenated rats causes neuronal necrosis. *Ann Neurol* 1985;18: 281–90.
9. Du F, Eid T, Lothman EW, et al. Preferential neuronal loss in layer III of the medial entorhinal cortex in rat models of temporal lobe epilepsy. *J Neurosci* 1995;15:6301–13.
10. Bertram EH, Lothman EW, Lenn NJ. The hippocampus in experimental chronic epilepsy: a morphometric analysis. *Ann Neurol* 1990;27:43–8.
11. Liu Z, Nagao T, Desjardins GC, et al. Quantitative evaluation of neuronal loss in the dorsal hippocampus in rats with long-term pilocarpine seizures. *Epilepsy Res* 1994;17:237–47.
12. Gorter JA, Van Vliet EA, Aronica E, et al. Progression of spontaneous seizures after status epilepticus is associated with mossy fibre sprouting and extensive bilateral loss of hilar parvalbumin and somatostatin-immunoreactive neurons. *Eur J Neurosci* 2001; 13:657–69.
13. Schmued LC, Albertson C, Slikker W Jr. Fluoro-Jade: a novel fluorochrome for the sensitive and reliable histochemical localization of neuronal degeneration. *Brain Res* 1997;751:37–46.
14. Lothman EW, Bertram EH, Bekenstein JW, et al. Self-sustaining limbic status epilepticus induced by "continuous" hippocampal stimulation: electrographic and behavioral characteristics. *Epilepsy Res* 1989;3:107–19.
15. Racine RJ. Modification of seizure activity by electrical stimulation, II: motor seizure. *Electroencephalogr Clin Neurophysiol* 1972;32:281–94.
16. Gavrieli Y, Sherman Y, Ben-Sasson SA. Identification of programmed cell death in situ via specific labeling of nuclear DNA fragmentation. *J Cell Biol* 1992;119:493–501.
17. Lucassen PJ, Chung WC, Vermeulen JP, et al. Microwave-enhanced in situ end-labeling of fragmented DNA: parametric studies in relation to postmortem delay and fixation of rat and human brain. *J Histochem Cytochem* 1995;43:1163–71.
18. English HF, Kyprianou N, Isaacs JT. Relationship between DNA fragmentation and apoptosis in the programmed cell death in the rat prostate following castration. *Prostate* 1989;15:233–50.
19. Lucassen PJ, Negoescu A, Labat-Moleur F, et al. Microwave enhanced in situ end labelling of apoptotic cells in tissue sections; pitfalls and possibilities. In: Shi SR, Gu J, Taylor CR, eds. *Antigen retrieval techniques.* Natick, Mass.: Eaton Publishing, 2000:71–91.
20. Amaral DG, Witter MP. Hippocampal formation. In: Paxinos G, ed. *The rat nervous system.* 2nd ed. London: Academic Press, 1995:443–93.
21. Paxinos G, Watson C. *The rat brain in stereotaxic coordinates*. San Diego: Academic Press, 1998.
22. Aronica E, Yankaya B, Troost D, et al. Induction of neonatal sodium channel II and III alpha isoform mRNAs in neurons and microglia after status epilepticus in the rat hippocampus. *Eur J Neurosci* 2001;13:1261–6.
23. Eriksson C, Van Dam AM, Lucassen PJ, et al. Immunohistochemical localization of interleukin-1beta, interleukin-1 receptor antagonist and interleukin-1beta converting enzyme/caspase-1 in the rat brain after peripheral administration of kainic acid. *Neuroscience* 1999;93:915–30.
24. Kubova H, Druga R, Lukasiuk K, et al. Status epilepticus causes necrotic damage in the mediodorsal nucleus of the thalamus in immature rats. *J Neurosci* 2001;21:3593–9.
25. Sato M, Chang E, Igarashi T, et al. Neuronal injury and loss after traumatic brain injury: time course and regional variability. *Brain Res* 2001;917:45–54.
26. Ingvar M, Morgan PF, Auer RN. The nature and timing of excitotoxic neuronal necrosis in the cerebral cortex, hippocampus and thalamus due to flurothyl-induced status epilepticus. *Acta Neuropathol* 1988;75:362–9.
27. Covolan L, Mello LE. Temporal profile of neuronal injury following pilocarpine or kainic acid-induced status epilepticus. *Epilepsy Res* 2000;39:133–52.
28. Poirier JL, Capek R, De Koninck Y. Differential progression of dark neuron and Fluoro-Jade labelling in the rat hippocampus following pilocarpine-induced status epilepticus. *Neuroscience* 2000; 97:59–68.
29. Tuunanen J, Lukasiuk K, Halonen T, et al. Status epilepticus-induced neuronal damage in the rat amygdaloid complex: distribution, time-course and mechanisms. *Neuroscience* 1999;94: 473–95.
30. Sloviter RS, Dean E, Sollas AL, et al. Apoptosis and necrosis induced in different hippocampal neuron populations by repetitive perforant path stimulation in the rat. *J Comp Neurol* 1996;366: 516–33.
31. Fujikawa DG, Shinmei SS, Cai B. Lithium-pilocarpine-induced status epilepticus produces necrotic neurons with internucleosomal DNA fragmentation in adult rats. *Eur J Neurosci* 1999;11:1605–14.
32. Roy M, Sapolsky R. Neuronal apoptosis in acute necrotic insults: why is this subject such a mess? *Trends Neurosci* 1999;22:419–22.
33. Kondratyev A, Gale K. Intracerebral injection of caspase-3 inhibitor prevents neuronal apoptosis after kainic acid-evoked status epilepticus. *Brain Res Mol Brain Res* 2000;75:216–24.
34. Mello LE, Covolan L. Spontaneous seizures preferentially injure interneurons in the pilocarpine model of chronic spontaneous seizures. *Epilepsy Res* 1996;26:123–9.
35. Pitkanen A, Nissinen J, Nairismagi J, et al. Progression of neuronal damage after status epilepticus and during spontaneous seizures in a rat model of temporal lobe epilepsy. *Prog Brain Res* 2002;135: 67–83.
36. Hopkins KJ, Wang G, Schmued LC. Temporal progression of kainic acid induced neuronal and myelin degeneration in the rat forebrain. *Brain Res* 2000;864:69–80.
37. Cavazos JE, Sutula TP. Progressive neuronal loss induced by kindling: a possible mechanism for mossy fiber synaptic reorganization and hippocampal sclerosis [published erratum appears in *Brain Res* 1991 Feb 8;541:179]. *Brain Res* 1990;527:1–6.
38. Zhang LX, Smith MA, Li XL, et al. Apoptosis of hippocampal neurons after amygdala kindled seizures. *Brain Res Mol Brain Res* 1998;55:198–208.
39. Mouritzen-Dam AM. Epilepsy and neuron loss in the hippocampus. *Epilepsia* 1980;21:617–29.
40. Fisher PD, Sperber EF, Moshe SL. Hippocampal sclerosis revisited. *Brain Dev* 1998;20:563–73.
41. Fernandez G, Effenberger O, Vinz B, et al. Hippocampal malformation as a cause of familial febrile convulsions and subsequent hippocampal sclerosis. *Neurology* 1998;50:909–17.
42. Jackson GD, Chambers BR, Berkovic SF. Hippocampal sclerosis: development in adult life. *Dev Neurosci* 1999;21:207–14.
43. Kalviainen R, Salmenpera T, Partanen K, et al. Recurrent seizures may cause hippocampal damage in temporal lobe epilepsy. *Neurology* 1998;50:1377–82.
44. O'Brien TJ, So EL, Meyer FB, et al. Progressive hippocampal atrophy in chronic intractable temporal lobe epilepsy. *Ann Neurol* 1999;45:526–9.
45. Tasch E, Cendes F, Li LM, et al. Neuroimaging evidence of progressive neuronal loss and dysfunction in temporal lobe epilepsy. *Ann Neurol* 1999;45:568–76.
46. Roch C, Leroy C, Nehlig A, et al. Magnetic resonance imaging in the study of the lithium-pilocarpine model of temporal lobe epilepsy in adult rats. *Epilepsia* 2002;43:325–35.
47. Liu RS, Lemieux L, Bell GS, et al. A longitudinal quantitative MRI study of community-based patients with chronic epilepsy and newly diagnosed seizures: methodology and preliminary findings. *Neuroimage* 2001;14:231–43.